This version of the article has been accepted for publication, after peer review, and is subject to Springer Nature's AM terms of use, but is not the Version of Record and does not reflect post-acceptance improvements or any corrections. The Version of Record is available online at: https://doi.org/10.1007/978-3-032-32230-2_36

Evaluating and Optimizing Fingertip-Free Cutaneous Haptics for Mixed Reality Interactions

Yannick Weiss[1] [0000−0003−1125−7963], Dennis Stanielewitz[2] [0009−0006−8726−8019], and Steeven Villa[3] [0000−0002−4881−1350]

[1] LMU Munich, Munich, Germany, yannick.weiss@ifi.lmu.de
[2] LMU Munich, Munich, Germany, stanielewitz@cip.ifi.lmu.de
[3] LMU Munich, Munich, Germany, villa@posthci.com

Abstract. Haptic feedback remains largely absent from mixed reality (MR) systems, despite its central role in everyday interaction. Many existing haptic approaches obstruct the fingertips or constrain movement, limiting their suitability for MR, where users must seamlessly interact with both virtual content and physical objects. We investigate an unobtrusive cutaneous approach that applies pressure and shear forces to the finger's proximal phalanx while leaving the fingertips free. We rebuild a haptic ring device and evaluate its effectiveness across common interaction widgets used in mid-air and with passive surface support. In an experimental user study with 24 participants, we systematically varied pressure and shear forces and modeled their effects on perceived pleasantness and realism using response surface methodology. Our results show that optimal haptic feedback varies by interaction: moderate shear improves mid-air tasks, stronger shear aids surface-supported widgets, and pressure mainly affects buttons. Trade-offs exist between pleasantness and realism, and passive surfaces substantially influence how active cutaneous cues are perceived. Overall, this work shows that fingertip-free cutaneous feedback can enhance a wide range of MR interactions without encumbering users' hands and highlights the importance of interaction-specific haptic tuning in MR systems.

Keywords: Cutaneous Feedback · Mixed Reality · Finger-Wearable.

1 Introduction

Haptic sensations are fundamental to everyday interaction, yet incorporating meaningful and realistic touch feedback into virtual reality (VR) and mixed reality (MR) systems remains challenging. Existing solutions range from grounded passive props [12] and encounter-type devices [18] to mobile wearable or handheld systems [5,21], but these typically constrain users' dexterity or isolate the interaction to the device itself. In contrast to conventional Augmented Reality (AR), which primarily overlays virtual content onto the real world, MR enables users to dynamically engage with both virtual and physical elements, including direct interaction with real objects augmented by virtual information and feedback.

This necessitates haptic technologies that do not obstruct natural movement, cover the entire sensing area, or interfere with interaction with real objects. As a result, most MR systems rely on free hand interaction without any haptic feedback, and fewer haptic devices have been adopted in MR [9,14,28], which still generally block the users' fingertips during interaction.

We instead build on a recent approach that provides haptic cues to the finger proximal phalanx (the bone segment of the finger closest to the hand) applied through a dynamic belt [20]. Prior work [29,24] has shown that this method can evoke sensations that users typically attribute to originate from their fingertip. This enables haptic feedback in MR [15] without restricting the user to virtual content and preserves natural interaction with physical objects, allowing them to be augmented with virtual sensations.

In this work, we rebuild and adapt this device to evaluate its effectiveness across a diverse set of pervasive interface building blocks in MR. We study its use in mid-air interaction as well as its combined use with passive feedback from a real physical surface. Using response surface methodology, we identify the optimal configurations of shear forces and pressure for each interaction type and provide paths for future development. With this, we contribute:

1. Findings of an empirical investigation of the device's capabilities for rendering realistic and pleasant haptic feedback across diverse MR interaction types.
2. A set of optimized rendering strategies for common interaction widgets along with guidance for future refinements based on response surface methodology.
3. Insights into the roles and interplay of active cutaneous rendering, passive haptics, and mid-air interactions in MR.

2 Active & Passive Haptic Rendering Approaches

Achieving realistic haptic feedback is a major challenge in immersive systems [31], which has motivated a large range of passive and active and approaches for haptic rendering. Passive haptics rely on static physical props without actuation to convey high-fidelity cues about shape, size, and material properties [1,12,32]. They are highly effective for representing pre-defined haptic characteristics and have shown to improve presence [12] and performance [32]. Especially in shared contexts, they have shown to be prominent as they can easily be distributed in the environment [4,11,23]. However, passive props are inherently inflexible: their position, geometry, and material properties cannot be easily modified. Active systems instead provide direct haptic rendering through the generation of kinesthetic and cutaneous cues, enabling dynamic and targeted control over sensations. Here, grounded force-feedback devices [16,17] can deliver highly precise and rapid kinesthetic feedback. But they severely restrict user movement and require constant contact with the end-effector. Encounter-type systems – in which a robotic actuator dynamically places a surface display in encountered areas – expand the interaction area and reduce the need for constant contact [18], though at the cost of reduced precision and speed. While these encountered-type systems preserve free-hand interaction, their reliance on external robotic infrastructure limits portability, scalability, and applicability in everyday MR scenarios, motivating interest in lightweight wearable alternatives. To support more mobile interactions and rapid actuation, many approaches for wearable devices have been proposed [21], ranging from entire exoskeletons [19], over haptic gloves [8,10,30], to fingertip-mounted actuators [25,26,27] that generally rely on cutaneous stimulation to substitute force cues [22]. Although these systems provide distributed feedback and mobility, they still rely on hardware that can obstruct natural interaction and limit the range of achievable haptic sensations. This is particularly problematic in MR scenarios, where users must interact with both virtual content and their physical environment. In such contexts, haptic feedback is confined to the specific device's capabilities, user interactions are constrained, and the user's hands may be visually occluded. As a result, relatively few approaches have been adapted and evaluated within augmented or MR settings [3]. These generally rely on fingertip-mounted devices producing cutaneous sensations through motor actuators [7,13], pneumatics [14], or hydraulics [9]. While these approaches show promise to extend haptic feedback capabilities to MR scenarios, they still obstruct the finger-tips, disallowing sensation of real objects and environments to be perceived. One approach is to retract the end-effector of the haptic device when not in use [28], enabling users to alternate between interaction with virtual and real content. However, this approach does not support simultaneous perception of both domains, limiting the ability to augment real-world objects and interactions.

Instead, we rely on an alternate established approach [15,20,24,29] which is mounted onto the finger's proximal phalanx, applying nominal and shear forces to the skin, while leaving the fingertips unoccupied. Prior investigation have shown this system, called hRing, to elicit sensations attributed to the fingertips [20] and that it can induce altered sensations of stiffness [29], friction [24], and shape [24] of objects. Additionally, prior work established its potential for augmented or mixed contexts due to its unobtrusive nature [15]. We extend on these works by exploring the interplay and resulting optimal configurations of shear forces and pressure for pleasant and realistic haptic experiences and the capabilities of the hRing to render realistic and congruent sensations for a variety of MR interactions both in mid-air and when augmenting a physical surface.

3 Study Design

We conducted a within-subject study investigating the use of the hRing haptic device [20] for a variety of interaction widgets in MR. Interactions were performed in mid-air, where feedback was provided solely by the haptic device, and on a flat physical surface, where fingertip contact with the table added passive haptics while the device remained active. This setup reflects MR, integrating virtual and physical haptic information within one interaction context. We systematically varied the applied pressure and shear forces during interaction with

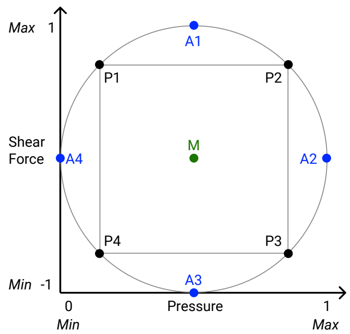

Fig. 1: Evaluated configurations of pressure and shear forces based on a Central Composite Design.

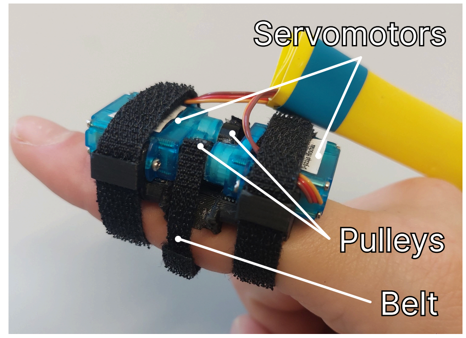

Fig. 2: Haptic ring consisting of two servomotors with pulleys that attach to an adjustable belt.

these widgets and captured participants' subjective ratings of their experience. We varied three variables:

Widget We evaluated a total of six different widgets, defined by the combination of widget type and interaction space: Button (Mid-Air), Button (Surface), Slider (Mid-Air), Slider (Surface), Knob (Mid-Air), and Knob (Surface). The buttons were activated by pressing downward with the index finger, the sliders by pinching between the index finger and thumb and translating horizontally, and the knobs by grasping and rotating clockwise or counter-clockwise. Interactions were performed either in mid-air, without physical support, or on a flat tabletop surface providing passive haptic feedback.

Pressure We varied the nominal forces the haptic device is applying to the finger in each trial. This is achieved by tightening the band through opposing movements of both attached motors.

Shear Force Additionally, we manipulated the shear forces applied to the finger by rotating the band through synchronous movements of motors. We varied both the amount of shear forces and their direction (either counter-clockwise or clockwise).

We treated every level of Widget as a separate block, counterbalancing them among participants using a Balanced Latin Square design. Within each block, we then varied the pressure and shear forces produced by the haptic device throughout multiple trials. To systematically investigate these continuous variables and potential optimal configurations, we employed a Central Composite Design (CCD), which allows the modeling of responses within our bounds of both dimensions. Specifically, we used an inscribed design to keep investigated points within our strict boundaries. For our two-dimensional CCD design, we evaluate 9 pre-defined points, illustrated in Figure 1: The center point (M) is replicated five times, which allows estimation of experimental reproducibility and systematic error. The factorial corner points (P1-P4) correspond to the vertices of a common

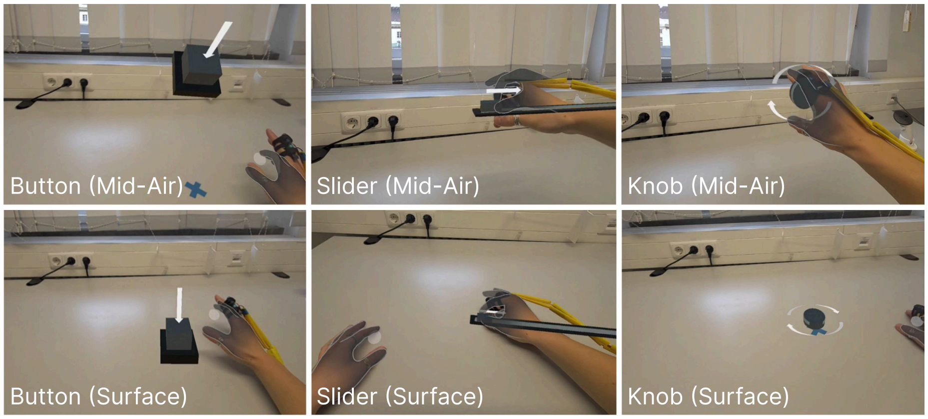

Fig. 3: Interactable widgets in mid-air and with a flat surface.

factorial system and provide the basis for estimating linear effects. The axial points (A1-A4) are located along a circle surrounding the factor cube and enable estimation of quadratic effects and potential curvature in the response surface. Zero magnitude for both pressure and shear forces was established individually for each participant during a calibration procedure and defined as the point at which the band first made contact with the skin. The maximum pressure (coded as 1) and shear forces (coded as -1 to 1) were determined individually by participants during calibration as the maximum magnitudes that still felt comfortable to them for prolonged use.

For each Widget block, we followed CCD procedure with the center point repeated every 3 steps (steps 1,4,7,10,13) and the other 8 points randomly assigned to the remaining steps in between. In total, each participants ran through 78 trials (6 Widget $\times$ 13 CCD Steps).

3.1 Task

In each trial, participants interacted with the interface widget using their right hand. For the button condition, participants pressed the button with their index finger until the widget turned green, indicating that the target distance had been reached. For the slider condition, participants grasped the slider with their index finger and thumb and translated it horizontally until the end position was reached. For the knob condition, participants grasped the knob with their index finger and thumb and rotated it clockwise. During the interaction movement, the haptic device generated pressure and shear forces, both starting at zero magnitude and increasing to the target value for the trial upon reaching the full interaction threshold. Once the target threshold was reached, participants could release the widget and lift their hand, after which the widget disappeared. The widgets were either displayed in mid-air, facing the participants, or overlaid onto a flat tabletop surface and oriented upward. In the tabletop condition, the participants' fingertips were in contact with the surface during interaction with the slider and knob, and at the end of the interaction for the button. After completing each trial, participants rated their experience using sliders displayed in mid-air in MR, which they could interact with using their free hand.

3.2 Apparatus

To apply variable nominal (pressure) and shear forces to participants' fingers and allow comparison, we reconstructed an established and evaluated haptic ring design from prior work [20,15,29,24]. The haptic ring is mounted onto the index-finger's proximal phalanx, leaving the fingertips unobstructed. It is comprised of two servomotors mounted in mirrored alignment, each with a pulley ($r = 4mm$) attached to the same Velcro band, which allows opposing or synchronous servo rotations to tighten (pressure) or rotate (shear forces) the band respectively. The device is secured using two additional static Velcro straps for the front and the back. The haptic ring is controlled through a microcontroller[4] attached to the forearm. The entire haptic device is displayed in Figure 2.

To interact with the widgets, participants wore a Meta Quest 3[5] head-mounted display (HMD). The virtual widgets were built in Unity3D[6] and overlaid over the camera-passthrough in real-time using the HMD's Mixed Reality passthrough feature. The interactable button, slider, and knob are displayed in Figure 3. White arrows indicated the direction the widgets could be interacted with. Once the targeted interaction thresholds has been reached, the widget turns green to signal completion and vanishes once the participant lifts their hand. Participants' hands were tracked using the HMD's in-built hand tracking and overlaid with a semi-transparent representation. To minimize potential confounding effects from servomotor noise or ambient environmental sounds, participants wore headphones playing white noise.

3.3 Measurements

We asked participants to rate their agreement with subjective statements on a continuous visual analog scale (VAS) from 0 (*Not at all*) to 1 (*Extremely*). Scales were presented directly in MR with a virtual slider. On the trial-level, we captured: PLEASANTNESS (*Experiencing the haptic sensations was pleasant to me*) and REALISM (*The haptic sensations resembled those I experience in real life*). After each completed CCD procedure (13 trials) for a widget, we additionally collected the perceived HAPTIC CONGRUENCY (*The haptic sensations integrated seamlessly with other senses.*) and VISUAL CONGRUENCY (*The visuals integrated seamlessly with other senses.*).

---

[4] Pimoroni Tiny2040, `https://shop.pimoroni.com/products/tiny-2040`, accessed: 2026-01-15

[5] `https://www.meta.com/quest/quest-3/`, accessed: 2026-01-14

[6] `https://unity.com/`, accessed: 2026-01-15

3.4 Procedure

We first welcomed participants and informed them about the study's goal, their task, and our data processing. After receiving written consent by participants, we asked them to fill out a small demographics questionnaire. Then, we helped participants equip the haptic device on the index finger of their right hand. We asked them to open and close their finger to confirm sufficient freedom of movement. Afterwards, they put on the HMD and calibrated the maximum constriction of the haptic device to a comfortable intensity. Participants first completed six training trials, each presenting one of the six virtual widgets without any haptic feedback from the device. Participants then put on the headphones and proceeded through the full set of 78 trials. The overall duration of the experiment was approximately one hour.

3.5 Participants

We recruited 24 participants through university channels. 9 described themselves as female, 14 as male, and one participant preferred not to say. Their age ranged from 19 to 35 years ($M = 25.29, SD = 4.31$). 22 participants were right-handed, while one identified as left-handed and another as ambidextrous/unsure. 18 participants had used MR previously (6 below 2 hours, 10 between 2 and 20 hours, and 2 for more than 20 hours). All participants had normal or corrected-to-normal vision and no known conditions affecting the haptic or tactile perception of their hands. We offered each participant 12€ or university course credit as compensation. This study was reviewed and approved by the ethics committee of our institution.

4 Results

In the following section, we present our results on widget-level ratings of visual and haptic congruency (subsection 4.1), as well as the response surfaces for each individual widget derived from our CCD design (subsection 4.2). For the response surfaces, we first describe the model selection based on lack-of-fit tests. We then conducted significance testing for each individual term of the final models, followed by finding optimal configurations within our tested design (constrained maximum) as well as determining the direction of most rapid increase in predicted ratings (steepest ascent).

4.1 Congruency Ratings

For the widget-level ratings of Haptic Congruency and Visual Congruency, we each fitted Linear Mixed Models (LMMs) by maximum likelihood (ML) using the `lme4` R-package [2]. We used the Widget as fixed effect and participants' unique IDs as random effect to account for interpersonal variability. For significance testing, we performed likelihood ratio tests (LRTs) comparing the full model to a null-model with only the random effect included.

Table 1: Means and standard deviations (SD) of haptic and visual congruency.

WIDGET	HAPTIC CONGRUENCY		VISUAL CONGRUENCY	
	Mean	SD	Mean	SD
Button (Mid-Air)	77.49	25.16	**77.71**	25.86
Button (Surface)	75.15	26.53	73.77	29.66
Slider (Mid-Air)	73.89	27.36	70.19	31.03
Slider (Surface)	**79.27**	23.46	77.27	26.80
Knob (Mid-Air)	71.29	26.44	70.16	26.20
Knob (Surface)	66.79	28.95	61.22	30.94

Mean ratings and standard deviations of all widgets are presented in Table 1. LRTs showed no significant effect of WIDGET ($\chi^2(5) = 7.53, p = 0.18$) on HAPTIC CONGRUENCY ratings. For VISUAL CONGRUENCY, LRTs revealed a significant main effect of WIDGET ($\chi^2(5) = 12.21, p = 0.03$). Post-hoc pairwise comparisons with Bonferroni correction showed a significant difference ($p < .05$) only between KNOB (SURFACE) and BUTTON (MID-AIR).

4.2 Response Surface Methodology

For trial-level ratings of PLEASANTNESS and REALISM, we performed RSM procedures for each widget separately. In addition to the separate PLEASANTNESS and REALISM ratings, we constructed a composite performance score by z-standardizing both ratings and weighting them equally, to identify configurations that jointly optimize both outcomes. For each widget and dependent variable, we then modeled the response based on the fixed factors of PRESSURE and SHEAR FORCE. We again fitted LMMs by ML with participants' IDs as random intercept to account for individual variability.

Model Selection For lack-of-fit tests, we modeled the fixed factors with a first-order (linear), second-order (quadratic), and third-order (cubic) function and conducted LRTs between each simpler and more complex model. A more complex model was only retained, if it significantly improved model fit over the lower-order one [6]. We found that the cubic model did not provide any significant improvement of fit over quadratic models for any WIDGET. The quadratic model significantly ($p < .05$) improved fit over the first-order model for the BUTTON (MID-AIR), KNOB (SURFACE), and SLIDER (MID-AIR) for all ratings (PLEASANTNESS, REALISM, and COMBINED) and for KNOB (MID-AIR) for PLEASANTNESS only. For these, we selected the quadratic model (Equation 2), while for the remainder, the simpler linear (Equation 1) model was sufficient. In the following equations p stands for PRESSURE and s for SHEAR FORCE.

$$F(x) = p + s \tag{1}$$

$$F(x) = p + s + p^2 + s^2 + (p * s) \tag{2}$$

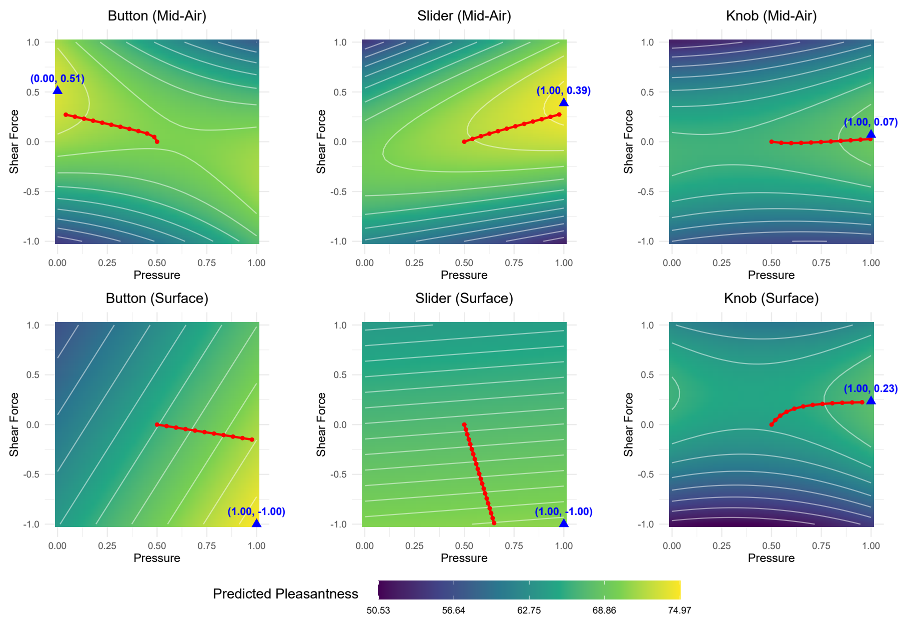

Fig. 4: Response surfaces for perceived Pleasantness displaying the variable's intensity (gradient), constrained maximum (▲), and steepest ascent (–).

Response Surface The modeled response surfaces of Pleasantness for each Widget are shown in Figure 4. We tested the significance of each term in the final models using LRTs comparing the full model with a reduced model with the individual fixed-effect term dropped out.

We found a significant effect of the linear term *pressure* on predicted Pleasantness for Button (Surface) ($\chi^2(1) = 5.70, p < .05$) and significant effect of the quadratic term $shearforce^2$ for Button (Mid-Air) ($\chi^2(1) = 7.04, p < .01$), Knob (Mid-Air) ($\chi^2(1) = 11.5, p < .001$), Slider (Mid-Air) ($\chi^2(1) = 13.4, p < .001$), and Knob (Surface) ($\chi^2(1) = 7.59, p < .01$).

The predicted responses for Realism are displayed in Figure 5. Here, LRTs revealed a significant effect in the second-order model for Knob (Surface) of both the linear term $shearforce$ ($\chi^2(1) = 7.11, p < .01$) and the quadratic term $shearforce^2$ ($\chi^2(1) = 8.90, p < .01$). Additionally, we found an effect of only the quadratic term $shearforce^2$ for Button (Mid-Air) ($\chi^2(1) = 10.2, p < .01$) and Slider (Mid-Air) ($\chi^2(1) = 17.7, p < .001$).

For the combined ratings (Combined), visualized in Figure 6, we found an effect of *pressure* in the Button (Surface) condition ($\chi^2(1) = 4.35, p < .05$), an effect of $shearforce$ in the Knob (Surface) condition ($\chi^2(1) = 4.35, p < .05$), and significant effects of $shearforce^2$ in the Button (Mid-Air) ($\chi^2(1) = 10.0, p < .01$), Knob (Mid-Air) ($\chi^2(1) = 9.16, p < .01$), Slider (Mid-Air) ($\chi^2(1) = 9.64, p < .01$), and Knob (Surface) ($\chi^2(1) = 18.8, p < .001$) conditions.

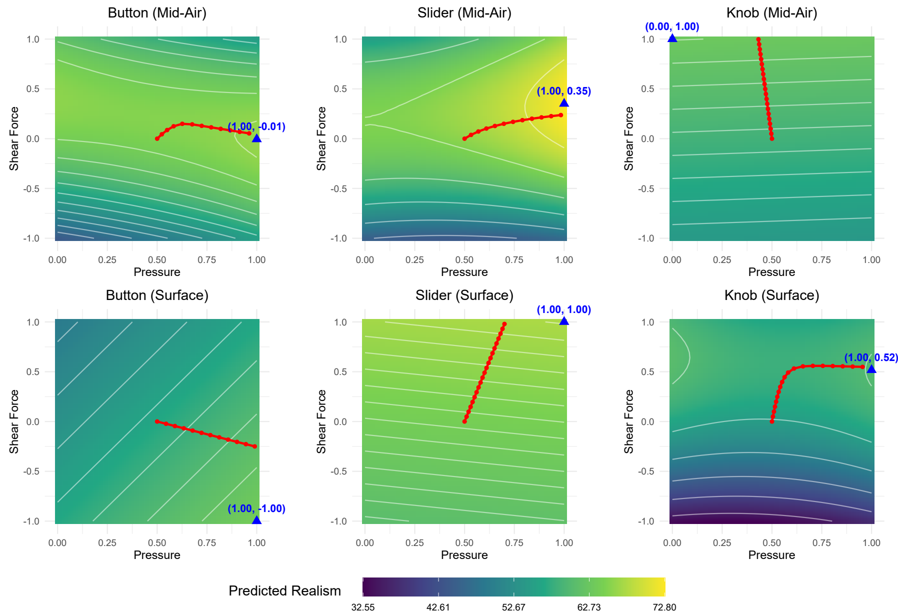

Fig. 5: Response surfaces for perceived Realism displaying the variable's intensity (gradient), constrained maximum (▲), and steepest ascent (–).

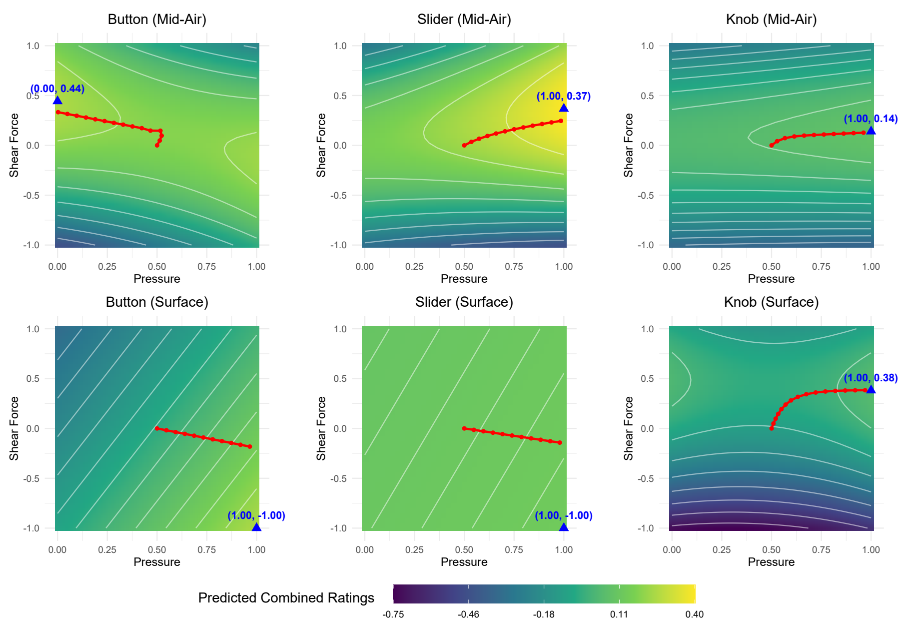

Fig. 6: Response surfaces for Combined Ratings displaying the variable's intensity (gradient), constrained maximum (▲), and steepest ascent (–).

Table 2: Predicted optimal values and corresponding configurations (p = PRESSURE, s = SHEAR FORCE) for PLEASANTNESS, REALISM, and COMBINED.

WIDGET	PLEASANTNESS		REALISM		COMBINED	
	Value	(p | s)	Value	(p | s)	Value	(p | s)
Button (Mid-Air)	73.53	(0.00|0.51)	66.37	(1.00|-0.01)	0.26	(0.00|0.44)
Button (Surface)	**74.97**	(1.00|-1.00)	64.00	(1.00|-1.00)	0.25	(1.00|-1.00)
Slider (Mid-Air)	74.55	(1.00|0.39)	**72.80**	(1.00|0.35)	**0.40**	(1.00|0.37)
Slider (Surface)	70.72	(1.00|-1.00)	67.56	(1.00|1.00)	0.13	(1.00|-1.00)
Knob (Mid-Air)	69.05	(1.00|0.07)	63.05	(0.00|1.00)	0.08	(1.00|0.14)
Knob (Surface)	67.84	(1.00|0.23)	60.26	(1.00|0.52)	0.05	(1.00|0.38)

Constrained Maximum To find optimal configurations of PRESSURE and SHEAR FORCE for our design, we computed maximum predicted points for PLEASANTNESS, REALISM, and COMBINED for each surface within covered boundaries. For this, we performed numerical optimization using R's `optim()` function with the `L-BFGS-B` method. Random effects were excluded from the predictions. The optimal points are highlighted for each WIDGET in Figure 4, Figure 5 and Figure 6 respectively. All optimal configurations and resulting predicted values for PLEASANTNESS, REALISM, and COMBINED are shown in Table 2. The optimally achievable predicted PLEASANTNESS ranges from 67.84 for KNOB (SURFACE) (at $pressure = 1$ & $shearforce = 0.23$) to 74.97 for BUTTON (SURFACE) (at $pressure = 1$ & $shearforce = -1$). For REALISM, the predicted optimal ratings range from 60.26 for KNOB (SURFACE) (at $pressure = 1$ & $shearforce = 0.52$) to 72.80 for SLIDER (MID-AIR) (at $pressure = 1$ & $shearforce = 0.35$). For COMBINED, optimal configurations reach scores of 0.05 for KNOB (SURFACE) (at $pressure = 1$ & $shearforce = 0.38$) to 0.40 for SLIDER (MID-AIR) (at $pressure = 1$ & $shearforce = 0.37$).

Steepest Ascent To determine the direction of increasing predicted responses, we first computed the stationary points of each quadratic model by solving the system where the gradient with respect to PRESSURE and SHEAR FORCE is zero. The type of each point was determined from the eigenvalues of the Hessian matrix. All stationary points within the observed predictor space were found to be saddle points, indicating that they are neither local maxima nor minima. Therefore, analogous to the linear models, the true maxima are likely located outside the observed boundaries.

To explore the direction of most rapid increase in predicted response, we computed steepest ascent paths. Starting from the center of the observed predictor space, we iteratively stepped in the normalized gradient direction of the predicted response. Gradients were computed using the fixed-effects portion of each model, including linear, quadratic, and interaction terms where present. Predicted responses along the paths were evaluated to illustrate how adjustments to PRESSURE and SHEAR FORCE could most effectively increase the predicted outcome. These paths are visualized in Figure 4, Figure 5 and Figure 6.

5 Discussion

The optimal balance of pressure and shear forces, as well as the maximum achievable pleasantness and realism, varied substantially across interaction widgets. This shows that no single optimal setting generalizes across interactions; instead, feedback magnitude and direction must be tuned to specific interaction types and use cases. Within our design range – constrained by individual comfort calibrations – the predicted optima and gradients shown in Figure 4, Figure 5, and Figure 6 provide guidance for reasonable configurations for established interactions.

For the combined metric (Combined), mid-air interactions exhibited strong curvature with respect to shear forces (see Figure 6 top), indicating that excessive shear in any direction eventually degrades experience. Nevertheless, constrained maxima and steepest ascent paths suggest that moderate positive shear generally improves combined ratings, implying that shear forces achievable and comfortable with our device are sufficient for mid-air interactions. In contrast, for surface-supported widgets (specifically the button and slider), ascent paths indicate that shear forces beyond our tested range could further improve scores. However, pleasantness and realism considered separately (Figure 4, Figure 5) reveal differing optimal shear directions, implying necessary design trade-offs.

Pressure had the strongest influence on pleasantness and realism for the Button (Surface). In most cases, ascent paths suggested optimal pressure magnitudes beyond our defined range, typically toward higher values. Exceptions were the Button (Mid-Air) and Knob (Mid-Air), where lower pressure improved respective pleasantness and realism ratings. While higher pressures are technically feasible, they must be applied cautiously: our bounds were based on individual comfort calibrations, and sustained increases may reduce comfort. Negative pressure is infeasible, but prior work [24] shows that sustained pressure followed by sudden release can evoke inverse sensations (e.g., softer virtual objects), suggesting a potential avenue for extending performance beyond our current thresholds.

Finally, the addition of passive surface feedback altered the acceptability of shear forces. While larger shear magnitudes reduced predicted ratings in mid-air interactions, they increased ratings for the Button (Surface) and Slider (Surface). The knob was an exception, receiving lower ratings overall, including reduced sensory congruency (subsection 4.1). We attribute this to increased interaction complexity: rotating both fingers while maintaining surface contact required whole-hand rotation rather than simple arm movement. Improving the knob interaction would likely require passive or active resistance towards its center, which is not supported by the current design and remains an area for future work.

Taken together, these findings should be interpreted in light of several considerations. While prior work has characterized the perceptual discriminability of normal and shear forces in isolation [20], the combined perception of these force components remains less well understood. Our results offer initial evidence of this interplay, but further systematic investigation is needed to better understand the underlying perceptual mechanisms. In addition, the parameter space was constrained by individual comfort thresholds, limiting the range of achievable forces despite potentially higher device capabilities. Objective performance metrics were not considered, as the simplicity of the interaction tasks was expected to yield minimal differences; however, such measures may be relevant for more complex scenarios as evidenced by prior work [15,20]. Finally, while this approach enabled the simultaneous perception of virtual and real haptic information through the active device and passive surface, further research is needed to determine how these findings generalize to other MR interactions involving everyday objects with diverse haptic characteristics.

6 Conclusion

We evaluated cutaneous haptic feedback for common MR interaction widgets in mid-air and with passive surface support. Using a within-subject experimental design with 24 participants and response surface methodology, we analyzed how pressure and shear forces applied to the proximal phalanx affect perceived pleasantness and realism of the feedback across interaction types. We show that optimal haptic configurations are strongly interaction-dependent, with no single setting generalizing across widgets. Moderate shear forces are sufficient and beneficial for mid-air interactions, while surface-supported widgets tend to benefit from larger shear forces, but may require trade-offs between pleasantness and realism. Pressure had the strongest influence for surface-based buttons, whereas lower pressure was preferred for some mid-air interactions.

Overall, this work demonstrates how cutaneous feedback can support diverse MR interactions without restricting natural hand use. Our findings and derived optimal configurations and trends provide practical guidance for MR haptic design and point to future improvements in device and interaction mechanisms.

7 Open Science

We make our project, dataset, and analysis scripts available in our OSF repository: `https://osf.io/5uw4h/`

Acknowledgments. This project is partially funded by the Deutsche Forschungsgemeinschaft (DFG, German Research Foundation) with the project-id: 521602817 as part of the Priority Program SPP2199 Scalable Interaction Paradigms for Pervasive Computing Environments. This project was partially funded by the European Research Council (ERC-2024-ADG) as part of the European Union's Horizon 2020 research and innovation program (grant agreement no. 101200584).

Disclosure of Interests. The authors have no competing interests to declare that are relevant to the content of this article.

References

1. Auda, J., Gruenefeld, U., Schneegass, S.: Enabling reusable haptic props for virtual reality by hand displacement. In: Proceedings of Mensch Und Computer 2021. p. 412–417. MuC '21, Association for Computing Machinery, New York, NY, USA (2021). https://doi.org/10.1145/3473856.3474000
2. Bates, D., Mächler, M., Bolker, B., Walker, S.: Fitting linear mixed-effects models using lme4. Journal of Statistical Software **67**(1), 1–48 (2015). https://doi.org/10.18637/jss.v067.i01
3. Bermejo, C., Hui, P.: A survey on haptic technologies for mobile augmented reality. ACM Comput. Surv. **54**(9) (Oct 2021). https://doi.org/10.1145/3465396
4. Cheok, A.D., Yang, X., Ying, Z.Z., Billinghurst, M., Kato, H.: Touch-space: Mixed reality game space based on ubiquitous, tangible, and social computing. Personal and Ubiquitous Computing **6**(5), 430–442 (Dec 2002). https://doi.org/10.1007/s007790200047
5. Choi, I., Ofek, E., Benko, H., Sinclair, M., Holz, C.: Claw: A multifunctional handheld haptic controller for grasping, touching, and triggering in virtual reality. In: Proceedings of the 2018 CHI Conference on Human Factors in Computing Systems. p. 1–13. CHI '18, Association for Computing Machinery, New York, NY, USA (2018). https://doi.org/10.1145/3173574.3174228
6. Dobson, A.J., Barnett, A.G.: An Introduction to Generalized Linear Models. CRC Press, Boca Raton, FL, USA (Apr 2018)
7. Gabardi, M., Solazzi, M., Leonardis, D., Frisoli, A.: A new wearable fingertip haptic interface for the rendering of virtual shapes and surface features. In: 2016 IEEE Haptics Symposium (HAPTICS). pp. 140–146 (2016). https://doi.org/10.1109/HAPTICS.2016.7463168
8. Gu, X., Zhang, Y., Sun, W., Bian, Y., Zhou, D., Kristensson, P.O.: Dexmo: An inexpensive and lightweight mechanical exoskeleton for motion capture and force feedback in vr. In: Proceedings of the 2016 CHI Conference on Human Factors in Computing Systems. p. 1991–1995. CHI '16, Association for Computing Machinery, New York, NY, USA (2016). https://doi.org/10.1145/2858036.2858487
9. Han, T., Anderson, F., Irani, P., Grossman, T.: Hydroring: Supporting mixed reality haptics using liquid flow. In: Proceedings of the 31st Annual ACM Symposium on User Interface Software and Technology. p. 913–925. UIST '18, Association for Computing Machinery, New York, NY, USA (2018). https://doi.org/10.1145/3242587.3242667
10. Hinchet, R., Vechev, V., Shea, H., Hilliges, O., Zurich, E.: Dextres: Wearable haptic feedback for grasping in vr via a thin form-factor electrostatic brake. The 31st Annual ACM Symposium on User Interface Software and Technology pp. 901–912 (2018). https://doi.org/10.1145/3242587.3242657
11. Huynh, D.N.T., Raveendran, K., Xu, Y., Spreen, K., MacIntyre, B.: Art of defense: a collaborative handheld augmented reality board game. In: Proceedings of the 2009 ACM SIGGRAPH Symposium on Video Games. p. 135–142. Sandbox '09, Association for Computing Machinery, New York, NY, USA (2009). https://doi.org/10.1145/1581073.1581095
12. Insko, B.E.: Passive Haptics Significantly Enhances Virtual Environments. Ph.D. thesis, The University of North Carolina at Chapel Hill (2001)
13. Kim, H., Kim, M., Lee, W.: Hapthimble: A wearable haptic device towards usable virtual touch screen. In: Proceedings of the 2016 CHI Conference on Human Factors

in Computing Systems. p. 3694–3705. CHI '16, Association for Computing Machinery, New York, NY, USA (2016). https://doi.org/10.1145/2858036.2858196, https://doi.org/10.1145/2858036.2858196
14. Kim, Y., Kim, S., Ha, T., Oakley, I., Woo, W., Ryu, J.: Air-jet button effects in ar. In: Pan, Z., Cheok, A., Haller, M., Lau, R.W.H., Saito, H., Liang, R. (eds.) Advances in Artificial Reality and Tele-Existence. pp. 384–391. Springer Berlin Heidelberg, Berlin, Heidelberg (2006)
15. Maisto, M., Pacchierotti, C., Chinello, F., Salvietti, G., De Luca, A., Prattichizzo, D.: Evaluation of wearable haptic systems for the fingers in augmented reality applications. IEEE Transactions on Haptics **10**(4), 511–522 (2017). https://doi.org/10.1109/TOH.2017.2691328
16. Martin, S., Hillier, N.: Characterisation of the novint falcon haptic device for application as a robot manipulator. In: Australasian Conference on Robotics and Automation (ACRA). pp. 291–292. Citeseer, Australian Robotics and Automation Association, Sydney, Australia (2009)
17. Massie, T.H., Salisbury, J.K., et al.: The phantom haptic interface: A device for probing virtual objects. In: Proceedings of the ASME winter annual meeting, symposium on haptic interfaces for virtual environment and teleoperator systems. vol. 55, pp. 295–300. Chicago, IL (1994)
18. Mercado, V.R., Marchal, M., Lecuyer, A.: "haptics on-demand": A survey on encountered-type haptic displays. IEEE Transactions on Haptics **PP**, 1–1 (2021). https://doi.org/10.1109/TOH.2021.3061150
19. Naik, P., Unde, J., Darekar, B., Ohol, S.S.: Pneumatic artificial muscle powered exoskeleton. In: Proceedings of the 2019 4th International Conference on Advances in Robotics. AIR '19, Association for Computing Machinery, New York, NY, USA (2020). https://doi.org/10.1145/3352593.3352627
20. Pacchierotti, C., Salvietti, G., Hussain, I., Meli, L., Prattichizzo, D.: The hring: A wearable haptic device to avoid occlusions in hand tracking. In: 2016 IEEE Haptics Symposium (HAPTICS). pp. 134–139 (2016). https://doi.org/10.1109/HAPTICS.2016.7463167
21. Pacchierotti, C., Sinclair, S., Solazzi, M., Frisoli, A., Hayward, V., Prattichizzo, D.: Wearable haptic systems for the fingertip and the hand: Taxonomy, review, and perspectives. IEEE Transactions on Haptics **10**(4), 580–600 (2017). https://doi.org/10.1109/TOH.2017.2689006
22. Prattichizzo, D., Pacchierotti, C., Rosati, G.: Cutaneous force feedback as a sensory subtraction technique in haptics. IEEE Transactions on Haptics **5**(4), 289–300 (2012). https://doi.org/10.1109/TOH.2012.15
23. Regenbrecht, H.T., Wagner, M., Baratoff, G.: Magicmeeting: A collaborative tangible augmented reality system. Virtual Reality **6**(3), 151–166 (Oct 2002). https://doi.org/10.1007/s100550200016
24. Salazar, S.V., Pacchierotti, C., de Tinguy, X., Maciel, A., Marchal, M.: Altering the stiffness, friction, and shape perception of tangible objects in virtual reality using wearable haptics. IEEE Transactions on Haptics **13**(1), 167–174 (2020). https://doi.org/10.1109/TOH.2020.2967389
25. Schorr, S.B., Okamura, A.M.: Fingertip tactile devices for virtual object manipulation and exploration. In: Proceedings of the 2017 CHI Conference on Human Factors in Computing Systems. p. 3115–3119. CHI '17, Association for Computing Machinery, New York, NY, USA (2017). https://doi.org/10.1145/3025453.3025744

26. Schorr, S.B., Quek, Z.F., Romano, R.Y., Nisky, I., Provancher, W.R., Okamura, A.M.: Sensory substitution via cutaneous skin stretch feedback. In: 2013 IEEE International Conference on Robotics and Automation. pp. 2341–2346. IEEE, New York, NY, USA (2013). https://doi.org/10.1109/ICRA.2013.6630894
27. Tao, Y., Teng, S.Y., Lopes, P.: Altering perceived softness of real rigid objects by restricting fingerpad deformation. In: The 34th Annual ACM Symposium on User Interface Software and Technology. p. 985–996. UIST '21, Association for Computing Machinery, New York, NY, USA (2021). https://doi.org/10.1145/3472749.3474800
28. Teng, S.Y., Li, P., Nith, R., Fonseca, J., Lopes, P.: Touch&fold: A foldable haptic actuator for rendering touch in mixed reality. In: Proceedings of the 2021 CHI Conference on Human Factors in Computing Systems. CHI '21, Association for Computing Machinery, New York, NY, USA (2021). https://doi.org/10.1145/3411764.3445099
29. de Tinguy, X., Pacchierotti, C., Marchal, M., Lécuyer, A.: Enhancing the stiffness perception of tangible objects in mixed reality using wearable haptics. In: 2018 IEEE Conference on Virtual Reality and 3D User Interfaces (VR). pp. 81–90 (2018). https://doi.org/10.1109/VR.2018.8446280
30. Vanichvoranun, N., Lee, H., Kim, S., Yoon, S.H.: Estatig: Wearable haptic feedback with multi-phalanx electrostatic brake for enhanced object perception in vr. Proc. ACM Interact. Mob. Wearable Ubiquitous Technol. **8**(3) (Sep 2024). https://doi.org/10.1145/3678567
31. Wee, C., Yap, K.M., Lim, W.N.: Haptic Interfaces for Virtual Reality: Challenges and Research Directions. IEEE Access **9**, 112145–112162 (2021). https://doi.org/10.1109/ACCESS.2021.3103598, conference Name: IEEE Access
32. White, M., Gain, J., Vimont, U., Lochner, D.: The case for haptic props: Shape, weight and vibro-tactile feedback. In: Motion, Interaction and Games. MIG '19, Association for Computing Machinery, New York, NY, USA (2019). https://doi.org/10.1145/3359566.3360058